HEFAT2007
5th International Conference on Heat Transfer, Fluid Mechanics and Thermodynamics
Sun City, South Africa
Paper number: KJ4

TRANSPORT AND DEPOSITION OF AEROSOLS IN HUMAN AIRWAYS

J. Katolicky, M. Forman, M. Jicha*
*Author for correspondence
Faculty of Mechanical Engineering,
Brno University of Technology,
Technicka 2, 61669 Brno, Czech Republic,
Email: jicha@fme.vutbr.cz

ABSTRACT

A numerical model of aerosol transport in human airways is presented that contains 6 to 9 bifurcations and about 100 terminations. The model was acquired from a CT scan of a living person and contains oral/nasal cavity, thoracic and lower airways. Two breathing activities are modeled: 1) Resting conditions with a tidal volume 0,5liter, the minute ventilation 15 l/min and the period 4 sec/cycle and 2) Heavy activity (maximum exercise) with the tidal volume 3.33 liter, the minute ventilation 120 l/min and the period 1.25 sec/cycle. The inspiration/expiration cycle was modeled following the sinusoidal function. Euler-Lagrange approach was used to model aerosol transport and deposition in the airways. The total concentration of aerosol was assumed 50μg/m^3 divided into three classes PM10, PM2.5 a PM 1 with appropriate fractions 25μg/m^3, 9 μg/m^3 and 16 μg/m^3, respectively. Results of the modeling show the velocity field in several locations along the airways in different time steps of inspiration and expiration phases as well as deposition of individual aerosol sizes in the individual segments of the human airways.

INTRODUCTION

Computational Fluid Dynamics simulation of airflow and particle transport and deposition in the human respiratory tract has been pursued by a number of researchers. Some recent examples (not exhaustive) are presented in [1, 2 and 3]. While CFD simulation of the nasopharynx/oropharynx have been quite successful [4], the complexity of the human tracheobronchial tree has defied detailed simulation of airflow in anything else than small sections, e.g. [5, 6].

PROBLEM DESCRIPTION AND FLOW CONFIGURATION

Computational modeling is performed of aerosol transport and deposition of three different size classes in the upper human airways down to 6th to 9th bifurcation. As a geometrical model, a High Resolution CT scan of a human was acquired from St. Anna University hospital in Brno – see Figure 1. The scan was transported into *.stl format, then smoothed and cleaned off unnecessary details and by means of an automatic mesh generator, first the surface and then the volume mesh were created.

NOMENCLATURE

t	[s]	Time
V	[liter]	Volume
x	[m]	Cartesian axis direction
y	[m]	Cartesian axis direction
z	[m]	Cartesian axis direction

Special characters

ω	[m]	frequency

Subscripts

t	Tidal (volume)

Figure 1 Picture of CT scan of airways

For the modeling purposes, the nasal/oral cavity was omitted and the inlet to the airways was placed above the glottis. The solution domain with selected planes in which results were analyzed is in Figure 2 (human front view). The model contains 3 millions of tetrahedral control volumes with high local refinement in locations of high velocity gradients. At the outlet, pressure conditions were ascribed. Commercial CFD code StarCD was used.

Two regimes, namely resting conditions and maximum exercise were simulated with the inlet conditions given in Tab.1. Both regimes were calculated in the transient mode inspiration /expiration that followed a sinusoidal curve according to the formula: $V(t) = V_t \sin(\omega t)$, where V_t is a tidal volume, ω is frequency and t is time. The total volume of the lungs from the CT scan was 4.1 liters.

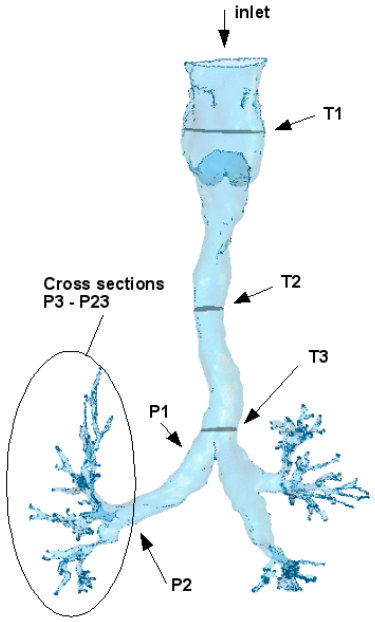

Figure 2 Picture of CT scan of airways (front view of the human)

Calculations were done using standard *k-ε* model of turbulence and Euler-Lagrange Eddy Interaction Model by Gosman and Ioannides [7] for particles transport; inlet conditions were ascribed as "inlet", outlet as pressure conditions with identical relative pressure in all airways terminations.

Tab.1 Modeling scenario

	Resting conditions	Maximum exercise
Tidal volume V_t [liter]	0.5	3.33
Flow rate [l/min]	7.5	120
Breathing frequency [Hz]	0.25	0.8
Period [s]	4	1.25

Three size classes of particles with different concentrations were assumed in the inlet to the trachea according to Tab. 2.

Tab.2 Aerosol characteristics

Particles diameter [μm]	Concentration [μg/m^3]
10	25
5	9
1	16

RESULTS AND THEIR DISCUSSION

Results show a slight asymmetry in the flow rate distribution between the left and right airways under both, the resting conditions and maximum exercise. The asymmetry can be seen in figures 3 and 4. The first generation corresponds to the planes P1, i.e. just the first bifurcation. The right side of the airways is in the figure on the left side (the front view of the human). At both regimes, the flow into the first generation is influenced by the flow pattern just behind the bend upstream in the plane marked T3 (see figure 2) that partially blocks the flow into the right airways. Thus we can see a lower flow rate into the right airways. The mass flow gradually decreases as the airways continue to bifurcate and distribute the air flow into the smaller airways.

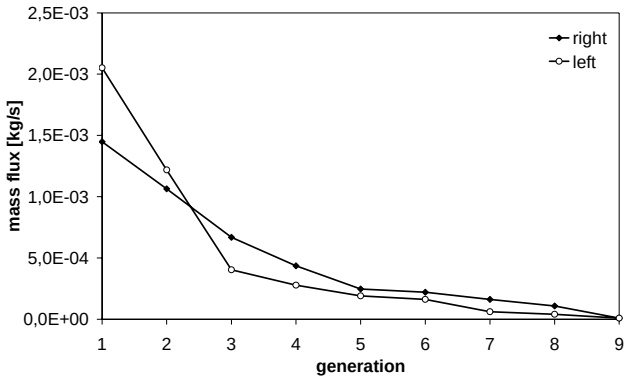

Figure 3 Mass flow rate for the maximum exercise

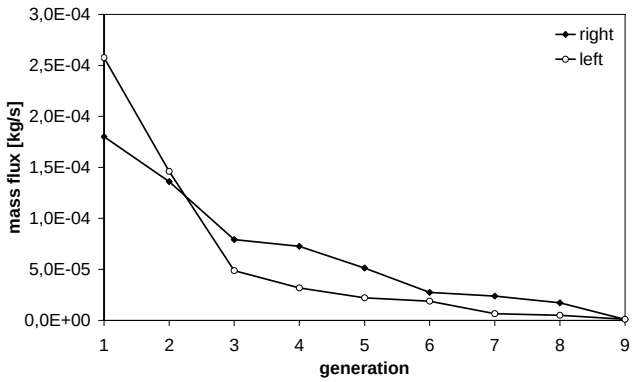

Figure 4 Mass flow rate for the resting conditions

In the figures 5 and 6, the Reynolds number is shown that reflects not only the flow rate of the air but also the influence of the diameter of the individual airways in the appropriate generations.

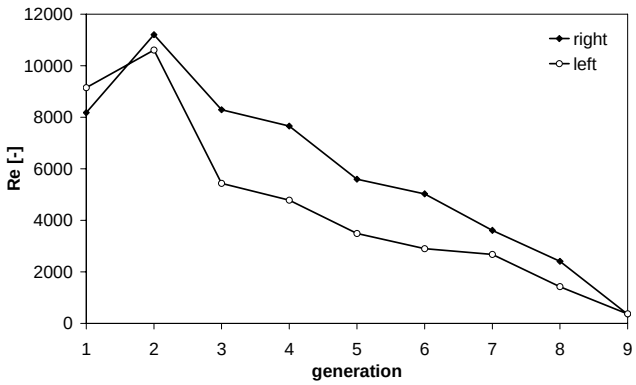

Figure 5 Reynolds number for the maximum exercise

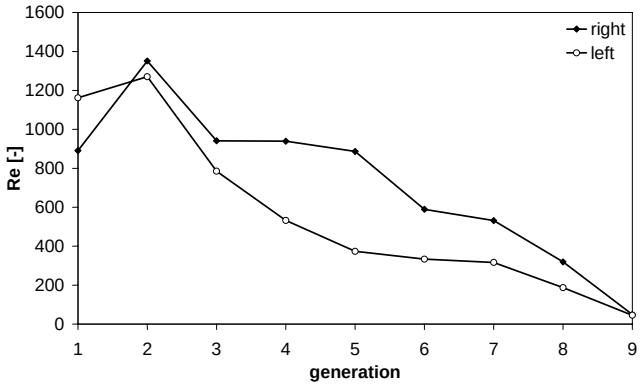

Figure 6 Reynolds number for he resting conditions

We can see an increase of the Reynolds number from the first to the second generation which is due to the increase of the velocity in the appropriate generation with the smaller cross section. This increase in the *Re* number can influence the deposition of aerosols due to changes in the turbulence and thus the aerosol transport characteristics. In the lower generations, the *Re* number gradually decreases due to both, the airflow rate and airways diameter reduction.

For the maximum exercise, the regime gradually changes from turbulent to laminar, but the CFD modeling was carried out for turbulent regime, which may influence the deposition of aerosols due to a higher lateral dispersion. In the future work, the authors will focus on the study of turbulence characteristics and the influence of turbulence model and changes in the turbulent characteristics on the aerosol transport and deposition.

Aerosol deposition is shown in figures 7 to 9.

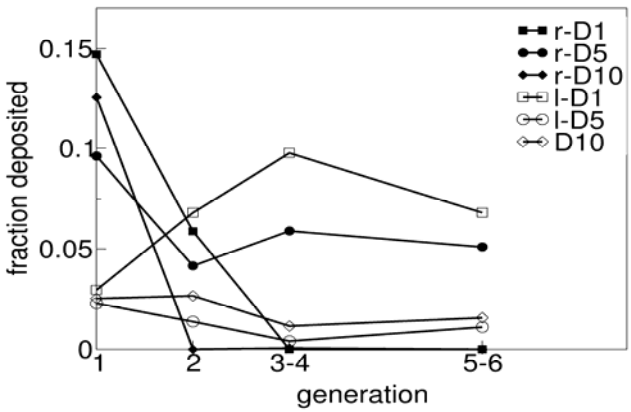

Figure 7 Deposition fraction of aerosols of PM1, PM5 and PM10 at the maximum exercise for the right (r) and left (l) airways

For the maximum exercise the highest deposition can be seen between the 1. and 2.bifurcation, i.e. in the airway of the 1.generation of the right airway. This can be explained by the flow pattern that forms behind the bend upstream the plane T3 (see the figure 2). There is a clear recirculation zone that forms in this location and which protrudes downstream thus enhancing the deposition of aerosols. This phenomenon also means that where an obstruction in the airways appears we can expect a more pronounced deposition. Highest deposition rate is shown for PM1 and PM10 in the 1.generation. Almost all PM10 deposit in the 1.generation and we can conclude that in this case it is the impaction that plays the major role. As for the high deposition of PM1, very probably the major part of small particles ends their life in the recirculation zone that forms behind the bend upstream the plane T3. Deposition of PM1 is almost accomplished in the 3. and 4.generation. As for the PM5, the deposition is more uniform and the most probable explanation is that the PM5 deposits mainly due to sedimentation. As for the left sided airways, the deposition of all PM is more uniform compared to the right sided airways. Again we can suspect that the flow pattern behind the bend upstream the plane T3 is responsible for the differences in the deposition. The left sided airways don't show so much directional changes as the right sided airways, that means the deposition by impaction doesn't appear so frequently and mainly the sedimentation is responsible for the deposition.

At the resting conditions, the deposition is lower than at the maximum exercise and shows a very different character. Deposition in the 1.generation is very low in both sides of airways. The character of the deposition rather shows on the sedimentation which could be expected due to a very low flow rate and particles velocity. Under such conditions the impaction is less significant and the deposition in the left and right airways is very similar each to other. The highest deposition rate is shown for PM1 in the 3. and 4.generation which could be attributed to the length of these generations which offer the sufficiently long residence time for the particles to settle down and to several local vortexes that trap the small particles and end their life.

Large part of aerosols leaves the airways at the terminating outlets without being deposited.

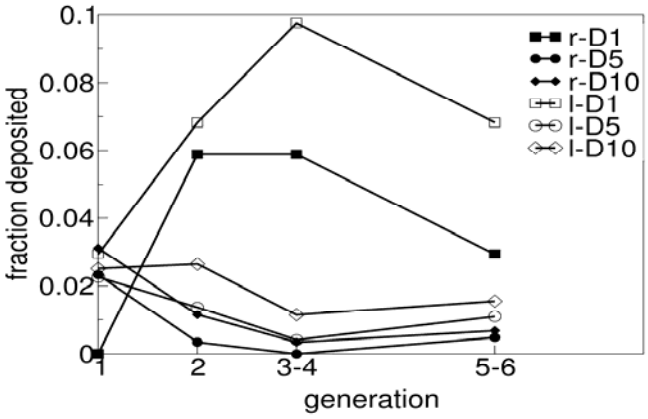

Figure 8 Deposition fraction of aerosols of PM1, PM5 and PM10 at the resting conditions for the right (r) and left (l) airways

The comparison between the resting conditions and the maximum exercise for both, the left and right airways is in the figure 9. For this graph we can see that the deposition is larger for the maximum exercise, except PM1, where the deposition shows a very similar rate. This is due to the fact that PM1 in the both sides, left and right airways deposit with a very similar rate due to sedimentation and capturing in the local vortexes. Higher deposition rate at the maximum exercise can be attributed to the higher role of the impaction that is higher at higher particles momentum. At the resting

conditions, it is the sedimentation that plays the major role (except the PM1 as explained above) in the deposition and thus the deposition is lower.

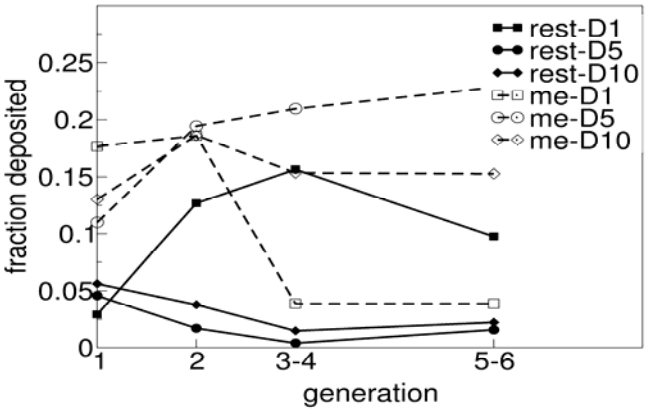

Figure 9 Total deposition fraction of aerosols of PM1, PM5 and PM10 for the resting conditions (rest) and the maximum exercise (me)

CONCLUSIONS

Computational modeling of the transport and deposition of aerosols of three size classes PM1, PM5 and PM10 was performed in the model of a respiratory tract acquired from the CT scan of a real human. The model contains 6 generations and isn't idealized as for the individual bifurcations. In this way the surface of the individual airways is not smooth, the individual generations have different cross sections that are not rounded but very different shape from each other. All these singularities result in more realistic results of the deposition.

We can conclude the following:

1. Aerosol deposition is influenced by local obstacles like bends, which results in different deposition rate. Local obstruction can create local vortexes in which smallest particles are trapped and end their life. Thus the deposition can be increased.
2. The deposition is also influenced by the asymmetry in the first bifurcation caused by an obstacle in the form of a bed, which results in different flow rates into the left and right airways and thus influences the whole process in the lower airways.
3. At the higher flow rate (maximum exercise) the major deposition mechanism is impaction for larger aerosols accompanied by the high deposition of smallest aerosols captured in the local vortexes.
4. In general, deposition is higher at the higher flow rate than at the lower flow rate. The major contribution to the deposition at the higher flow rate is impaction that is accompanied by the sedimentation.

ACKNOWLEDGMENT

Financial support from the Czech Ministry of Education and Youth through the COST project 1P05OC028 is gratefully acknowledged.

REFERENCES

[1] Balashazy, I., Heistracher, T. and Hofman, W., 1996, Airflow and particle deposition patterns in bronchial airway bifurcation: the effect of different CFD models and bifurcation geometry, J. Aerosol Med. 9:287-301.

[2] Edwards, D.A., 1996, Numerical simulation of air and particle transport in the conducting airways, J. Aerosol Med. 9:303-316.

[3] Sarangapani, R. and Wexler, A., 1999, Modelling aerosol bolus dispersion in human airways, J. Aerosol Sci. 30:1345-162.

[4] Matida, E.A., Finlay, W.H., Lange, C.F. and Grgic, B., 2002, Improved numerical simulation of aerosol deposition in a idealized mouth-throut, J. Aerosol Sci. 35:1-19.

[5] Zhang, Z., Kleinstreuer, C., Kim, C.S. and Hickey, A.J., 2002, Aerosol transport and deposition in a triple bifurcation bronchial airway model with local tumor, Inhalation Toxicology, 14:1111-1133.

[6] Comer, J.K., Kleinstreuer, C. and Kim, C.S, 2000, Aerosol transport and deposition in sequentially bifurcating airways, J. Biomechanical Eng., 122:152-158.

[7] Gosman, A.D. and Ioannides, E., 1981, Aspects of computer simulation of liquid fueled combustors, Paper AIAA-81-0323, 19th Aerospace Science Meeting, St. Louis, MO.